

# Latest results from Tevatron collider experiments

A. V. Popov,<sup>\* a†</sup>

<sup>a</sup> *Institute for High Energy Physics  
Protvino, Russia*

## Abstract

This article reviews some of the latest results from Tevatron Collider experiments, using up to  $6 \text{ fb}^{-1}$  of integrated luminosity collected with the DØ and CDF detectors.

## 1 Introduction

In this article we will describe some of the newest results obtained by DØ and CDF experiments in 2009-2010. We will present in turn some results about Higgs boson (Standard Model and beyond) searches, electroweak physics, QCD physics, b physics and new phenomena searches.

The Tevatron is a  $p\bar{p}$  collider located near Chicago with a center-of-mass energy of 1.96 TeV. The peak instantaneous luminosity (as of spring 2010) is  $\sim 4 \cdot 10^{32} \text{ cm}^{-2}\text{sec}^{-1}$  and, at the middle of May 2010, the accumulated luminosity delivered to the experiments reached  $8.6 \text{ fb}^{-1}$  mark. The Tevatron is running very stable, it is in stores almost 120 hours per week and gives to the experiments additional 50-60  $\text{pb}^{-1}$  of delivered luminosity per week.

The DØ and CDF experiments are two  $4\pi$  multi-purpose detectors taking data at the Tevatron Collider and they are, in some sense, complementary to each other. The DØ detector contains a silicon and fiber tracking detector at the most central part, which allows to measure precisely the location and momentum of charged particles. The tracking detector is surrounded by a solenoid which delivers a magnetic field of 2 T. The compensating, finely segmented, liquid argon and uranium calorimeter provides nearly a full solid angle coverage up to a rapidity larger than 4. The muon detector is composed of the central muon proportional drift tubes, scintillating detectors used in the trigger and mini-drift tubes and scintillating detectors in the forward region, allowing a muon detection up to a rapidity of 2. A toroid magnet allows to reconstruct the muon momentum using the muon system only, and a better resolution is obtained by combining this information with the ones from the tracking detectors. The CDF detector has similar performance and is composed of a central tracking and silicon detector, a calorimeter made of lead sheets sandwiches with scintillator for the electromagnetic part, and of iron plates and scintillator for the hadronic part, and a muon detector. The resolution of the CDF tracking detector is larger than for DØ because of the space availability and it also has a capability to trigger on tracks at Level 1 (i.e. synchronous with the bunch crossing) and to identify and trigger on tracks displaced with respect to the primary vertex at Level 2. The DØ detector has a finer calorimeter segmentation and a muon system extending farther forward.

The detectors collect data with an efficiency of  $\sim 90\%$ . The small inefficiency is partly due to a deadtime coming from the trigger and Data Acquisition and partly to operational constraints. At the middle of May 2010  $\sim 7.7 \text{ fb}^{-1}$  were written to tape by each experiment. However, in the following, we will present results obtained with up to  $\sim 6 \text{ fb}^{-1}$  statistics.

---

\***e-mail:** Alexei.Popov@ihep.ru

†for the CDF and DØ Collaborations

## 2 Higgs boson searches at the Tevatron

The standard model of particle physics has been remarkably successful in interpreting existing experimental data. However, the electroweak symmetry breaking of the model remains to be understood. In the model, the symmetry is postulated to be spontaneously broken through the so-called Higgs mechanism [1]. As a result, a neutral scalar fundamental particle called the Higgs boson is predicted to exist. Searching for this elusive particle has been a major undertaking of the experimental particle physics community over the last two decades.

With the exception of its mass, the couplings of the Higgs boson to fermions and gauge bosons are theoretically well known. Its mass, however, can be inferred from precision measurements of electroweak data, as the Higgs boson often appears in the loops of high-order electroweak corrections. A recent global fit to precision electroweak data yields a central value for the Higgs boson mass of  $84_{-26}^{+34}$  GeV and a 95 % C.L. upper bound of 154 GeV [2]. Direct searches at LEP have set a lower bound of 114.4 GeV and, if we take this result into account in global fit, upper bound of 185 GeV, again at 95 % C.L. [3].

The relatively low mass preferred by the fit is encouraging for the search for and potential discovery of the Higgs boson at the Fermilab Tevatron collider. At the Tevatron, the Higgs boson can be produced through the following four processes (ordered in decreasing cross section):  $gg \rightarrow H$ ,  $q\bar{q} \rightarrow WH$ ,  $q\bar{q} \rightarrow ZH$  and  $q\bar{q} \rightarrow qqH$ . Since it couples to other particles in proportion to the mass of the particle, the Higgs boson decays predominantly to the heaviest particle kinematically allowed. Thus in the low mass region of  $114 < m_H \lesssim 130$  GeV, Higgs decays mostly to  $b\bar{b}$ , while for masses above 130 GeV,  $H \rightarrow WW$  decay dominates.

The minimal extension of the standard model, the minimal supersymmetric standard model (MSSM), predicts five Higgs bosons: two CP even ( $h, H$ ) and one CP odd ( $A$ ) neutral bosons as well as two charged bosons ( $H^+$  and  $H^-$ ) [4]. Two of the three neutral bosons are generally degenerate in mass and are often collectively denoted as  $\phi$ . Two main production processes for  $\phi$  at the Tevatron are  $b\bar{b} \rightarrow \phi$  and  $gg \rightarrow \phi$ . Their cross sections are proportional to  $\tan^2\beta$ , here  $\tan\beta$  is the ratio of the vacuum expectation values of the two Higgs doublet fields in the model. Thus, at high  $\tan\beta$ , the cross section could be large. Moreover,  $\phi$  decays mostly to  $b\bar{b}$  and  $\tau\tau$ . At  $\tan\beta \approx 40$ , for example,  $Br(\phi \rightarrow b\bar{b}) \approx 90\%$  and  $Br(\phi \rightarrow \tau\tau) \approx 10\%$ .

In this article we will pay attention to the Standard Model Higgs searches both in low and high mass sectors, as well as some results from MSSM Higgs searches.

### 2.1 Associated production $q\bar{q} \rightarrow WH, ZH$

Though the  $gg \rightarrow H$  production dominates over the entire mass region of interest at the Tevatron, the large  $H \rightarrow b\bar{b}$  decay branching ratio at low masses renders it impractical for the search in this mass region, due to an overwhelming QCD  $b\bar{b}$  background. Consequently searches at low masses are generally focused on Higgs productions in association with vector bosons such as  $WH$  and  $ZH$ . The decays of  $W \rightarrow l\nu$  and  $Z \rightarrow ll, \nu\nu$  lead to distinct signatures for triggering and identification while  $H \rightarrow b\bar{b}$  decay provides the benefit of the Higgs mass reconstruction.

The  $WH \rightarrow l\nu b\bar{b}$  final state is one of the most sensitive channels in the 115–130 GeV mass range. It is characterized by one high  $p_T$  lepton, a large missing transverse energy and a pair of b-jets. Both CDF and DØ recently presented the results of the analysis for this channel based on the statistics around  $5 \text{ fb}^{-1}$  [5]. Unfortunately, there are no any excesses of events over the standard model prediction and an upper cross section limit is from 3 to 7 times higher (at  $m_H = 115$  GeV) than the standard model value for the cross section.

The  $ZH \rightarrow ll b\bar{b}$  process in principle provides the cleanest Higgs signature since every final-state object can be reconstructed. Unfortunately even for a Higgs process, the rate for this process is low. CDF has analyzed  $4.1 \text{ fb}^{-1}$  of the data, DØ has analyzed a dataset of similar size ( $4.2 \text{ fb}^{-1}$ ) [6]. At  $m_H = 115$  GeV, the observed upper limit in CDF is 5.9 times of the standard model value and the limit observed in DØ is 9.1 times of the standard model value.

The signature of  $ZH \rightarrow \nu\nu b\bar{b}$  final state is two b-jets and large missing transverse energy. This process has a bigger cross section in compare to  $llb\bar{b}$  signature, but also significantly larger multijet background. Another feature of this analysis is that it is found to be also sensitive to  $WH \rightarrow l\nu b\bar{b}$  with unidentified lepton. In fact, the  $WH$  and  $ZH$  contribute almost equally to the final signal yield. DØ analyzed  $5.2 \text{ fb}^{-1}$  of the data, CDF -  $3.6 \text{ fb}^{-1}$  [7]. The observed upper limit for  $m_H = 115 \text{ GeV}$  are 3.7 (DØ) and 6.1 (CDF) times the expected standard model cross section.

## 2.2 $H \rightarrow WW$

For a Higgs mass above 130 GeV, the  $g\bar{g} \rightarrow H$  production followed by the  $H \rightarrow WW \rightarrow l\nu l\nu$  decay offers the most promise for a potential Higgs discovery at the Tevatron, as backgrounds are strongly suppressed by the presence of two high  $p_T$  leptons and a large missing transverse energy. Compared with searches for a low mass Higgs, the direct reconstruction of Higgs mass in this final state is unfortunately infeasible due to the two undetected neutrinos. However, the final result shows that this drawback is well compensated by the cleanliness of the event topology. Both CDF and DØ have analyzed up to  $5.4 \text{ fb}^{-1}$  ( $4.8 \text{ fb}^{-1}$  for CDF and  $5.4 \text{ fb}^{-1}$  for DØ) of the data for this final state and made a combination of their results to improve the sensitivity [8]. No excess is observed above background expectation, and resulting limits on Higgs boson production exclude a standard-model Higgs boson in the mass range 162-166 GeV (159–169 GeV with expected limit) at the 95% C.L. This is the first direct constraint on the mass of the Higgs boson beyond that obtained at LEP.

## 2.3 Combined limits for standard model Higgs boson

To arrive at a Tevatron limit on the Higgs production for a given mass, results from CDF and DØ experiments are combined, taking into account correlations in systematic uncertainties. For this combination 90 (35 for CDF, 54 for DØ) final states with Higgs decay modes  $H \rightarrow b\bar{b}$ ,  $H \rightarrow WW$ ,  $H \rightarrow \tau\tau$  and  $H \rightarrow \gamma\gamma$  were used with up to  $5.4 \text{ fb}^{-1}$  of data [9]. The 95 % upper limits on Higgs boson production are a factor of 2.70 (0.94) times the standard model cross section for  $m_H = 115$  (165) GeV (see Fig. 1).

## 2.4 Searches for supersymmetric Higgs bosons

While searches for a standard model Higgs boson have the spotlight, both experiments have significant efforts in searches for the supersymmetric Higgs bosons as well. Ongoing analysis include  $gb \rightarrow \phi b \rightarrow b\bar{b}b$ ,  $bb \rightarrow \phi \rightarrow \tau\tau$  and  $gb \rightarrow \phi b \rightarrow \tau\tau b$ . First process has a large probability due to large  $Br(\phi \rightarrow b\bar{b})$ , but QCD background is also large. Background is reduced for the second process, but  $Br(\phi \rightarrow \tau\tau)$  is significantly smaller than  $Br(\phi \rightarrow b\bar{b})$ .

CDF recently presented a search for neutral Higgs bosons decaying into  $b\bar{b}$ , produced in association with  $b$  quarks, using a data sample corresponding to  $2.5 \text{ fb}^{-1}$  of integrated luminosity [10]. The obtained expected and observed limits are plotted as a function of the Higgs mass in Figure 2. Note a positive deviation of greater than  $2\sigma$  from the expectation in the mass region of 130-160 GeV.

In MSSM scenario this analysis allows exclusion of  $\tan\beta$  values greater than 40 for  $m_H = 90 \text{ GeV}$  and about 100-120 for the mass range 110-170 GeV.

The Tevatron combination on the search for a neutral Higgs boson in the  $\tau\tau$  final state using  $1.8 \text{ fb}^{-1}$  and  $2.2 \text{ fb}^{-1}$  of integrated luminosity collected at the CDF and DØ experiments was also recently presented [11]. CDF took into account  $gg \rightarrow \phi$  and  $b\bar{b} \rightarrow \phi$  production, while at DØ only  $gg \rightarrow \phi$  was taking into account. No excess of events over standard model prediction was observed and, in MSSM interpretation,  $\tan\beta$  values greater than 30 for  $m_H = 130\text{--}150 \text{ GeV}$  were excluded.

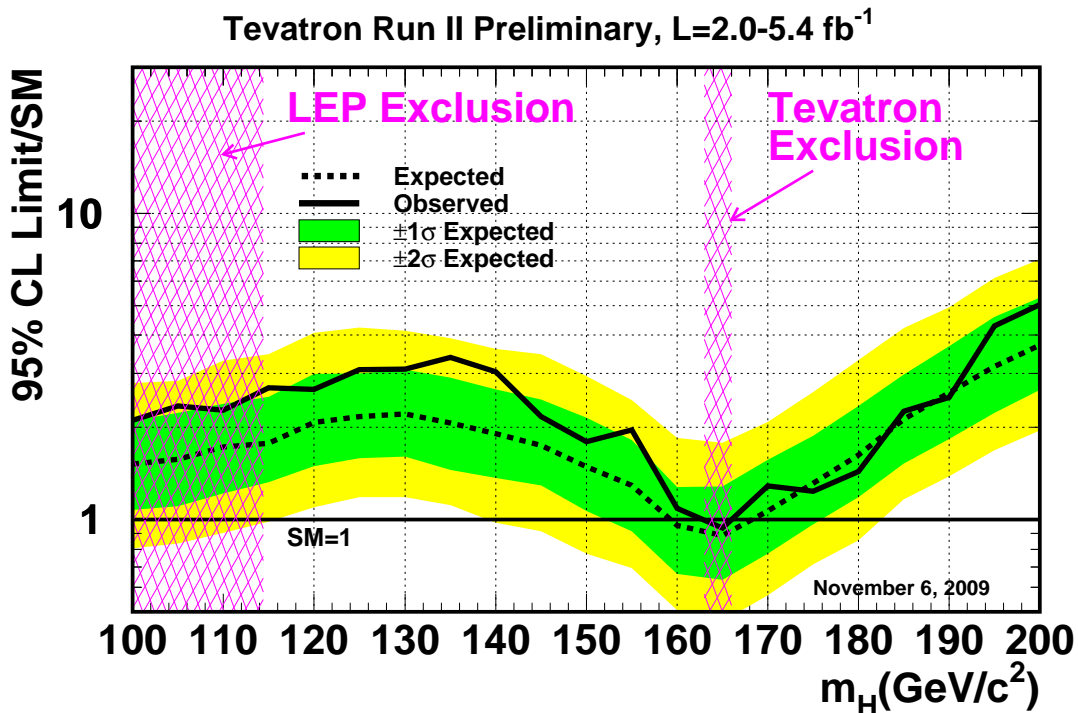


Figure 1: Observed and expected (median, for the background-only hypothesis) 95% C.L. upper limits on the ratios to the SM cross section, as functions of the Higgs boson mass for the combined CDF and  $D\bar{O}$  analyses. The limits are expressed as a multiple of the SM prediction for test masses (every 5 GeV) for which both experiments have performed dedicated searches in different channels. The points are joined by straight lines for better readability. The bands indicate the 68% and 95% probability regions where the limits can fluctuate, in the absence of signal.

### 3 Electroweak and QCD physics

Many different analysis on electroweak and QCD physics are progressing at the Tevatron, only a very small fraction of them is mentioned in this article.

#### 3.1 W boson mass and width measurements

$W$  and  $Z$  bosons are mainly produced via quark-antiquark annihilations at the Fermilab Tevatron collider. Precision measurements with these gauge bosons provide us with high precision tests of the Standard Model as well as indirect search for possible new physics beyond the Standard Model.

In the standard model,  $M_W$  can be calculated using the electromagnetic coupling constant  $\alpha$ , the Fermi constant  $G_F$  and the weak mixing angle  $\sin^2\theta_W$ . It also receives quantum radiative corrections that depend on the top quark mass and the SM Higgs boson mass. A precise measurement of  $M_W$  thus can be used to make constraints on the Higgs mass. To make the equal contribution to the Higgs mass uncertainty, we need to have  $\Delta M_W \approx 0.006 \times \Delta M_{top}$ . With the current world average value of  $\Delta M_{top} = 1.3$  GeV and  $\Delta M_W = 0.025$  GeV,  $\Delta M_W$  is the limiting factor for the Higgs mass constraint.

CDF and  $D\bar{O}$  experiments recently reports the combination of the  $W$  mass and width

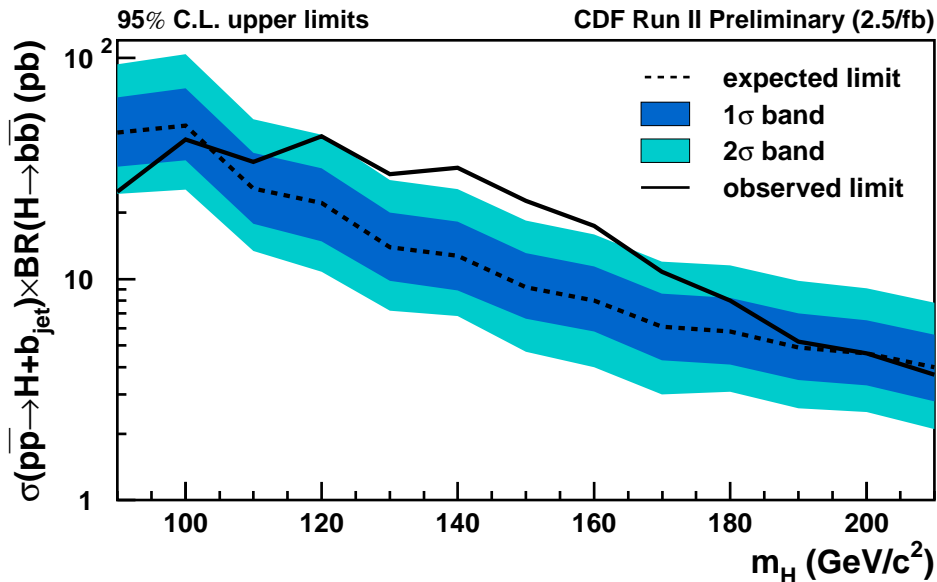


Figure 2: Median,  $1\sigma$ , and  $2\sigma$  expected limits, and observed limits versus  $m_H$

measurements, taken into account statistical and systematic uncertainties as well as correlations among systematic uncertainties [12]. The combined Tevatron result for the mass of the  $W$  is  $M_W = 80.420 \pm 0.031$  GeV. For the first time the total uncertainty of 31 MeV from the Tevatron is smaller than that of 33 MeV from LEP II [13]. The combination of the new Tevatron result with the LEP II preliminary result, assuming no correlations, yield the world average  $M_W = 80.399 \pm 0.023$  GeV (Figure 3). The combined CDF and DØ result for the width of the  $W$  boson is  $\Gamma_W = 2085 \pm 49$  MeV, leading to the new world average  $\Gamma_W = 2085 \pm 42$  MeV, which is in agreement with SM prediction of  $\Gamma_W = 2093 \pm 2$  MeV (Figure 4) [14].

### 3.2 Double parton interactions

Many features of high energy inelastic hadron collisions depend directly on the parton structure of hadrons. The inelastic scattering of nucleons need not to occur only through a single parton-parton interaction and the contribution from double parton (DP) collisions can be significant. The rate of events with multiple parton scatterings depends on how the partons are spatially distributed within the nucleon. DP cross sections can be expressed as  $\sigma_{DP} \equiv m \frac{\sigma_A \sigma_B}{2 \cdot \sigma_{eff}}$ , where  $\sigma_A$  and  $\sigma_B$  are the cross sections of two independent partonic scatterings  $A$  and  $B$ . The factor  $m$  is equal to unity when processes  $A$  and  $B$  are indistinguishable while  $m = 2$  otherwise. The process independent scaling parameter  $\sigma_{eff}$  has the units of cross section. The ratio  $\sigma_B / \sigma_{eff}$  can be interpreted as the probability for partonic process  $B$  to occur provided that process  $A$  has already occurred. If the partons are uniformly distributed inside the nucleon (large  $\sigma_{eff}$ ),  $\sigma_{DP}$  will be rather small and, conversely, it will be large for a highly concentrated parton spatial density (small  $\sigma_{eff}$ ).

In addition to constraining predictions from various models of nucleon structure and providing a better understanding of non-perturbative QCD dynamics, measurements of  $\sigma_{eff}$  are also needed for the accurate estimation of backgrounds for many rare new physics processes as well as for Higgs boson searches at the Tevatron and LHC.

DØ has studied  $\gamma + 3$ -jet events to measure double parton scattering and  $\sigma_{eff}$  and its possible dependence from  $p_T$  of the jet in the second interaction [15]. The values of  $\sigma_{eff}$  in different jet  $p_T$  bins agree with each other within their uncertainties and reveal a mean of  $\sigma_{eff} = 16.4 \pm 0.3(stat.) \pm 2.3(syst.)$  mb.

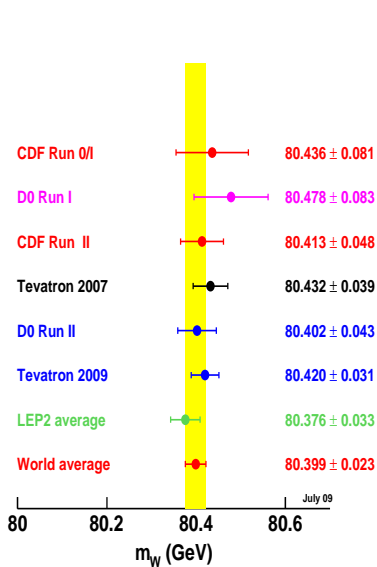


Figure 3: Summary of the measurements of the  $W$  boson mass and their average as of July 2009. An estimate of the world average of the Tevatron and LEP results assuming no correlations between the Tevatron and LEP is included.

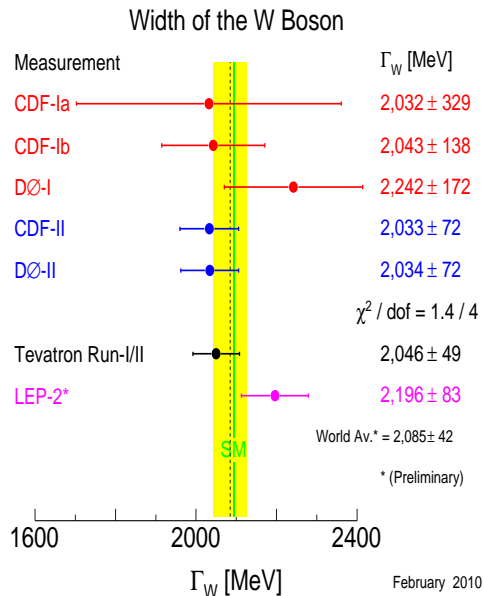


Figure 4: Comparison of measurements of the width of the  $W$ -boson and their average. The most recent preliminary result from LEP2 and the Standard Model prediction are also shown. The Tevatron values are corrected for small inconsistencies in theoretical assumptions among the original publications.

### 3.3 Di-jet angular distributions

At large momentum transfers, dijet production has the largest cross section of all processes at a hadron collider and therefore directly probes the highest energy regime. It can be used to test the standard model at previously unexplored small distance scales and to search for signals predicted by new physics models. The angular distribution of dijets with respect to the hadron beam direction is directly sensitive to the dynamics of the underlying reaction. While in quantum chromodynamics (QCD) this distribution shows small but noticeable deviations from Rutherford scattering, an excess at large angles from the beam axis would be a sign of new physics processes not included in the SM, such as substructure of quarks (“quark compositeness”), or the existence of additional compactified spatial dimensions (“extra dimensions”).

DØ measured dijet angular distributions with the data sample corresponds to an integrated luminosity of  $0.7 \text{ fb}^{-1}$  [16]. The result of this measurements is presented on Figure 5. Dijet angular distributions have been measured over a range of dijet masses, from 0.25 TeV to above 1.1 TeV. The data are in good agreement with the predictions of perturbative QCD and are used to constrain new physics models including quark compositeness, large extra dimensions, and  $\text{TeV}^{-1}$  scale extra dimensions. The lower limit on quark compositeness energy scale parameter is found to be  $\Lambda > 2.9 \text{ TeV}$ , the lower limit on effective Planck scale  $M_S$  for ADD LED model and GRW formalism is  $M_S > 1.66 \text{ TeV}$  and for HLZ formalism with number of extra dimensions  $n_d = 3$   $M_S > 1.97 \text{ TeV}$ . For  $\text{TeV}^{-1}$  model the lower limit on compactification scale parameter  $M_C > 1.59 \text{ TeV}$  was obtained.

## 4 B-physics

The measurement of the CP violation in the  $b$ -meson system and of  $b$ -meson rare decays provides information about the electroweak symmetry breaking in terms of flavour structure

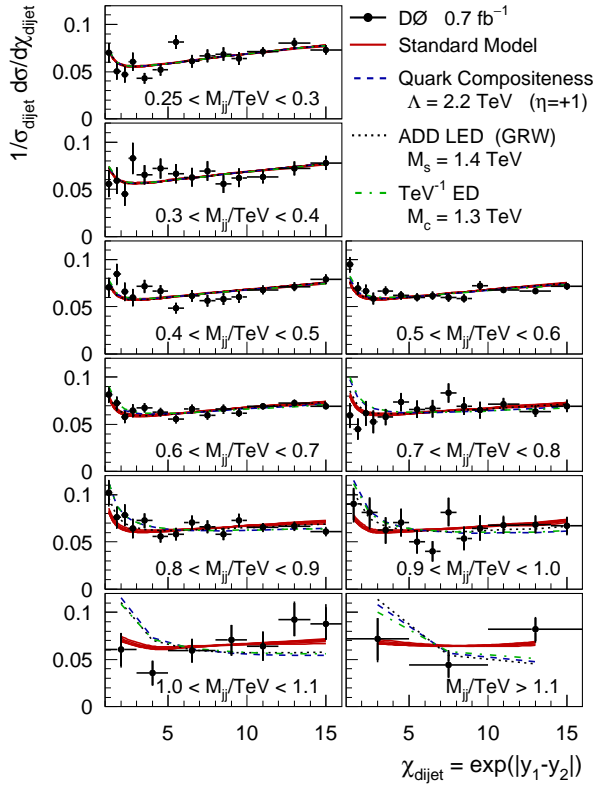


Figure 5: Normalized differential cross sections in  $\chi_{dijet}$  compared to standard model predictions and to the predictions of various new physics models. The error bars display the quadratic sum of statistical and systematic uncertainties. The standard model theory band includes uncertainties from scale variations and PDF uncertainties. The rapidity  $y$  is defined as  $y = 0.5 \ln[(1 + \beta \cos \theta)/(1 - \beta \cos \theta)]$ .

of the CKM matrix and flavour changing neutral currents. The deviation of the experimental observations from the Standard Model predictions allows to constrain new physics.

#### 4.1 $B_{s,d}^0 \rightarrow \mu\mu$

In the standard model, Flavor Changing Neutral Current (FCNC) decays are highly suppressed and can only occur through higher order loop diagrams. The decay rate for the FCNC decay  $B_s^0 \rightarrow \mu^+\mu^-$  is proportional to the CKM matrix element  $|V_{ts}|^2$ , while the rate of  $B_d^0 \rightarrow \mu^+\mu^-$  decays is proportional to  $|V_{td}|^2$ . Both rates are further suppressed by helicity factors. The SM expectations for these branching fractions are  $Br(B_s^0 \rightarrow \mu^+\mu^-) = (3.86 \pm 0.57) \times 10^{-9}$  and  $Br(B_d^0 \rightarrow \mu^+\mu^-) = (1.00 \pm 0.14) \times 10^{-10}$  [17], which are one order of magnitude smaller than the current experimental sensitivity. However, new physics contributions can significantly enhance these branching fractions. An observation of these decays at the Tevatron would be unambiguous evidence for physics beyond the SM.

CDF and D0 presented the results of the analysis, based on the  $3.7 \text{ fb}^{-1}$  (CDF) and  $5 \text{ fb}^{-1}$  (D0) data sets [18]. The upper limit on  $Br(B_s^0 \rightarrow \mu^+\mu^-)$  measured by the two experiments is  $4.3 \times 10^{-8}$  (CDF) and  $5.3 \times 10^{-8}$  (D0) at 95% C.L. For  $B_d^0 \rightarrow \mu^+\mu^-$  decay corresponding upper limit is  $7.6 \times 10^{-9}$  (CDF). The result is in agreement with the SM.

#### 4.2 CP violation in di-muon charge asymmetry measurement

Studies of particle production and decay under the reversal of discrete symmetries (charge, parity and time reversal) have yielded considerable insight on the structure of the theories that describe high energy phenomena. Of particular interest is the observation of CP violation,

a phenomenon well established in the  $K^0$  and  $B_d^0$  systems, but not yet observed for the  $B_s^0$  system, where all CP violation effects are expected to be small in the standard model (SM). The violation of CP symmetry is a necessary condition for baryogenesis, the process thought to be responsible for the matter-antimatter asymmetry of the universe. However, the observed CP violation in the  $K^0$  and  $B_d^0$  systems, consistent with the standard model expectation, is not sufficient to explain this asymmetry, suggesting the presence of additional sources of CP violation, beyond the standard model. One of the sensitive way to discover "anomalous" CP violation is a charge asymmetry measurements.

DØ recently reported the new result of the di-muon charge asymmetry measurements obtained with a total data set of  $6.1 \text{ fb}^{-1}$  [19]. The measured value is  $A_{sl}^b \equiv \frac{N_b^{++} - N_b^{--}}{N_b^{++} + N_b^{--}}$  - like sign dimuon charge asymmetry of semileptonic  $B$  decays, where one muon in the like sign pair comes from direct semileptonic decay  $b \rightarrow \mu^- X$ , while other muon comes from direct semileptonic decay after neutral B mixing:  $B^0 \rightarrow \bar{B}^0 \rightarrow \mu^- X$ . Non zero value of  $A_{sl}^b$  means that the semileptonic decays of  $B^0$  and  $\bar{B}^0$  are different. It can occur only due to CP violation in mixing in the B systems. The standard model prediction for this asymmetry is  $(2.3_{-0.6}^{+0.5}) \times 10^{-4}$  which is well below the sensitivity of current experiments.

The analysis is performed on two data samples. The inclusive muon sample is composed of events with at least one single muon candidate passing the muon selection and at least one single muon trigger. The like-sign di-muon sample consists of all events with at least two muons candidates of the same charge that pass the dimuon selection and at least one dimuon trigger. This analysis relies on:

- Reversing of the polarity of the toroidal and solenoidal magnet every two weeks, in order to cancel first order effects related with the instrumental asymmetry.
- Measurement of background contribution to the asymmetry. Muons are considered from the decay of charged kaons and pions and punch-through kaons, pions and protons. The contribution of these backgrounds to the asymmetry  $a$  and  $A$  are extracted directly from data.

The quantities  $a \equiv \frac{n^+ - n^-}{n^+ + n^-}$ , where  $n^\pm$  is the number of positive and negative identified muons, and  $A \equiv \frac{N^{++} - N^{--}}{N^{++} + N^{--}}$ , where  $N^{\pm\pm}$  is the number of like sign muon pairs, are extracted respectively from the inclusive and like-sign sample. The value of  $A_{sl}^b$  is extracted independently from  $A$  and  $a$  according to the relations  $a = k \times A_{sl}^b + a_{bkg}$  and  $A = K \times A_{sl}^b + A_{bkg}$ , where  $a_{bkg}$  and  $A_{bkg}$  are the background contributions extracted from data and  $k$  and  $K$  are scale factors estimated in MC.

The measured like sign dimuon asymmetry is  $A_{sl}^b = -0.00957 \pm 0.00251(stat) \pm 0.00146(syst)$  (Figure 6). This asymmetry is in disagreement with the prediction of the SM by  $3.2\sigma$  deviation. This is the first evidence of anomalous CP-violation in the mixing of neutral B-mesons.

## 5 New Phenomena searches

The Standard Model (SM), although phenomenologically successful, leaves many questions unanswered. To address some of these questions, new models and theories have been devised that need to be confirmed with experimental facts. The Tevatron plays an important role in the quest of phenomena Beyond the Standard Model (BSM).

There are many BSM searches currently progressing at the Tevatron including supersymmetry, leptoquarks of all three generations, technicolor, large extra dimensions, compositeness, extra gauge bosons, model independent searches (MIS) to name a few. In this article we will look on the recent results concerning the leptoquarks and extra gauge bosons searches.



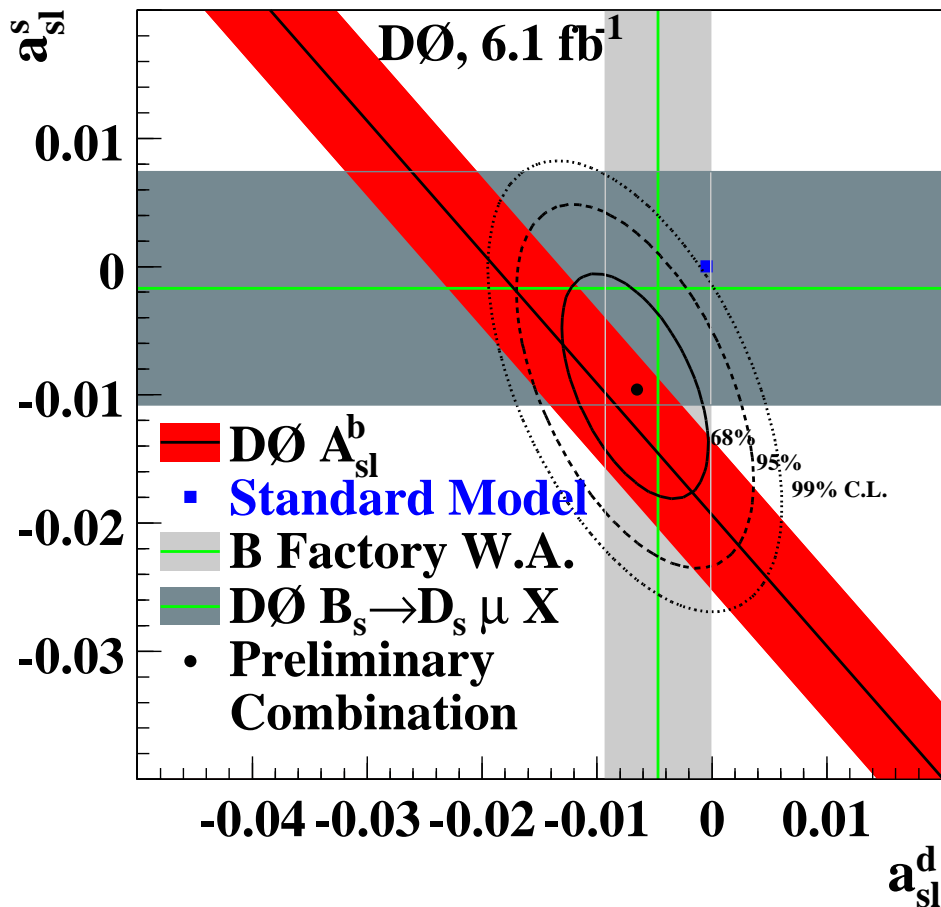


Figure 6: The comparison of the like-sign dimuon charge asymmetry  $A_{sl}^b$  measured by DØ and the SM is shown. Also shown are the existing measurements of  $a_{sl}^d$  and  $a_{sl}^s$ .  $A_{sl}^b$  is found with a deviation of  $3.2\sigma$  from the SM.

### 5.1 $3^{rd}$ generation leptoquarks search

Leptoquarks (LQ) are exotic particles that have color, electric charge, and both lepton and baryon numbers and appear in extended gauge theories and composite models. Current theory suggests that leptoquarks would come in three different generations corresponding to the three quark and lepton generations. Charge 1/3 third generation leptoquarks would decay into either a  $\tau$  neutrino plus a  $b$  quark or, if heavy enough, to a  $\tau$  lepton plus a  $t$  quark. Leptoquarks can be either scalar or vector particles. This analysis sets limits for scalar leptoquarks for which the cross section is lower and computed to higher order in perturbation theory. At the Tevatron, leptoquarks would be produced mainly through  $q\bar{q}$  annihilation or  $gg$  fusion.

DØ reported the new result of the  $3^{rd}$  generation leptoquark searches obtained with a total data set of  $4 \text{ fb}^{-1}$  [20]. Final state with missing transverse energy and two  $b$  quarks was studied. Such a state could result from either third generation leptoquark pair production ( $LQ_3 \rightarrow \nu b$ ) or, in MSSM interpretation, from scalar bottom quark pair production ( $\tilde{b}_1 \rightarrow b\tilde{\chi}_1^0$ , where  $\tilde{\chi}_1^0$  is the lightest neutralino). As the result of this analysis third generation scalar leptoquarks with  $M_{LQ} < 252 \text{ GeV}$  were excluded at the 95% C.L. Also, 95% C.L. limits in the  $(m_{\tilde{b}_1}, m_{\tilde{\chi}_1^0})$  mass plane was set, improving previous Tevatron result (see Figure 7).

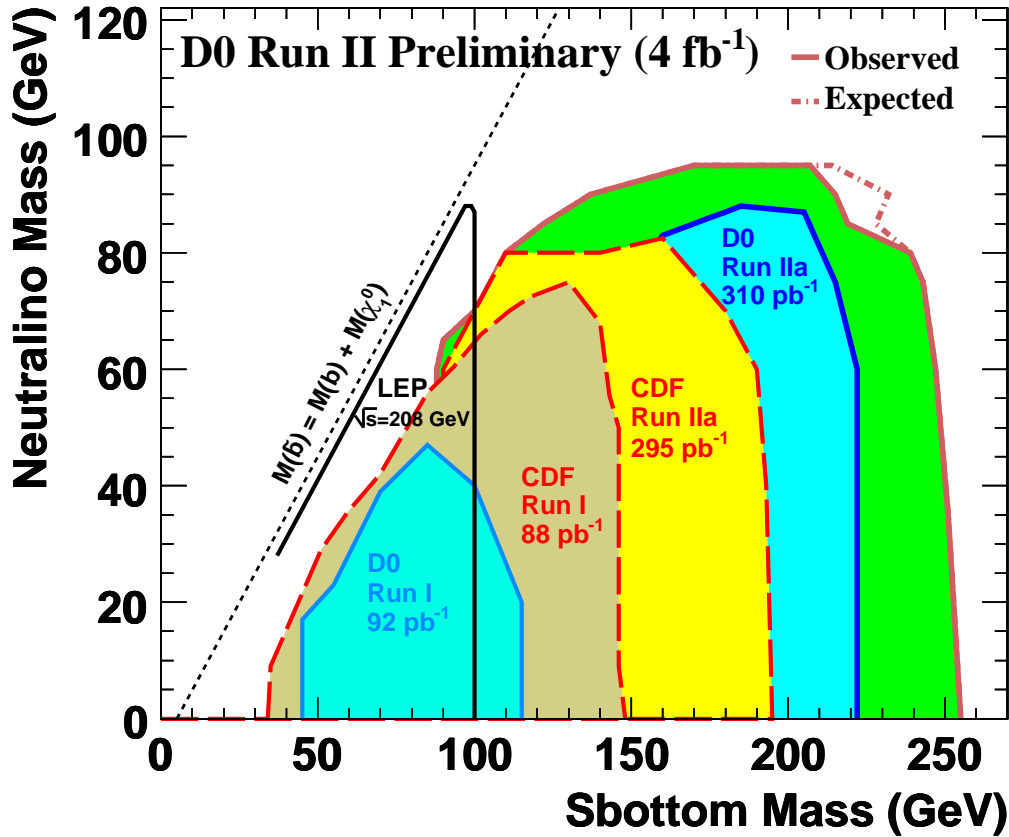


Figure 7: The 95% C.L. exclusion contour in  $(m_{\tilde{b}_1}, m_{\tilde{\chi}_1^0})$  mass plane. Also presented results from previous searches at LEP and at the Tevatron.

## 5.2 $WW$ and $WZ$ resonances

Many extensions of the SM, such as the sequential standard model (SSM), extra dimensions, little Higgs, and technicolor models, predict new heavy  $W'$  resonances decaying to a pair of electroweak  $W$  and  $Z$  bosons. Some models also offer an alternative to the SM mechanism of electroweak symmetry breaking. Thus, the observation of resonant  $WZ$  boson production would not only manifest new physics beyond the SM, but also could yield an insight into the origin of mass.

DØ experiment recently published the result of a search for a heavy charged boson, referred to as the  $W'$ , decaying to  $W$  and  $Z$  bosons using  $4.1 \text{ fb}^{-1}$  of integrated luminosity [21]. The  $WZ$  pairs are reconstructed through their decays into three charged leptons ( $l = e, \mu$ ). A total of 9 data events is observed in good agreement with the background prediction.  $W'$  with masses between 188 and 520 GeV was excluded at the 95% C.L. within a SSM interpretation (Figure 8). This result can be also interpreted with a technicolor model, where particles such as  $\rho_T$  and  $a_T$  have narrow widths and can decay to  $WZ$  bosons. The experimental signature of this particles is therefore similar to that of a  $W'$ . The results of this analysis were interpreted within the low-scale technicolor model, where the masses of  $\rho_T$  and  $a_T$  are predicted to be below 500 GeV, well within the energy reach of the Tevatron.  $\rho_T$  with mass between 208 and 408 GeV was excluded at 95% C.L. (see Figure 9).

CDF also reports on a search for resonances decaying into a pair of gauge bosons,  $W^+W^-$  or  $W^\pm Z^0$  based on  $2.9 \text{ fb}^{-1}$  data set [22]. In this search mode, one  $W$  decays through a leptonic (electron) mode and the other boson decays into two jets. Three resonance hypotheses,  $G^*$  (Randall-Sundrum graviton),  $Z'$  and  $W'$  are tested and mass region exclusions  $M(G^*) < 607$

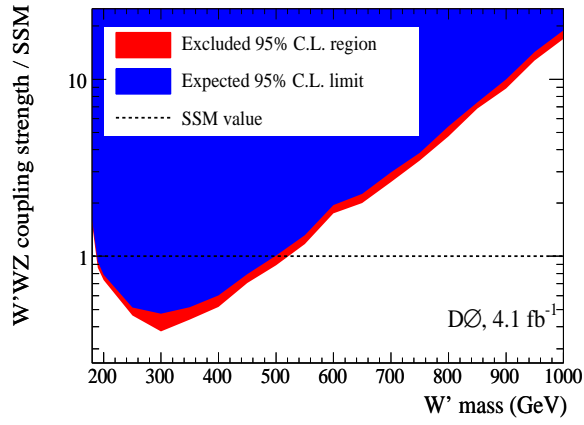


Figure 8: Expected and excluded area of the  $W'WZ$  coupling strength normalized to the SSM value as a function of the  $W'$  mass

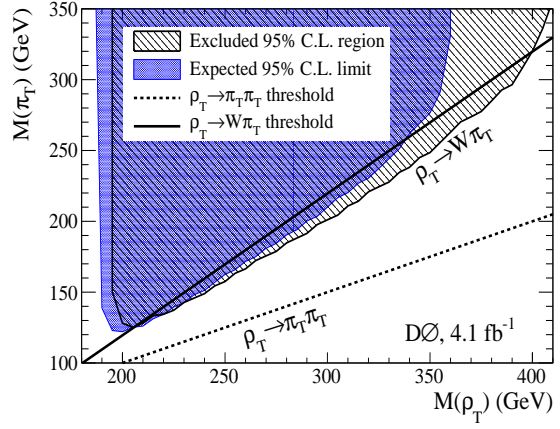


Figure 9: Expected and excluded areas of the  $\pi_T$  vs.  $\rho_T$  masses are given with the thresholds of the  $\rho_T \rightarrow W\pi_T$  and  $\rho_T \rightarrow \pi_T\pi_T$  overlaid

GeV,  $247 < M(Z') < 545$  GeV and  $284 < M(W') < 515$  GeV were obtained at 95% C.L.

## 6 Summary

Tevatron collider is performing extremely well, delivering up to  $70 \text{ pb}^{-1}$  of data per week to the experiments. Currently Tevatron run is expected to proceed at least till late 2011 and we expect to reach  $12 \text{ fb}^{-1}$  mark in terms of integrated luminosity and discussion of the extension of the Tevatron run for another few years is in progress. CDF and DØ experiments are collecting and analysing data smoothly and with high efficiency, many discoveries and precision measurements were already published, more than 200 studies are in progress now, publishing 1–2 papers per week. We already have some hints of the physics beyond the standard model, one of the latest examples is "anomalous" like sign dimuon charge asymmetry, which was mentioned earlier in this article. Also Higgs boson searches are in a very active stage, for the first time after LEP the new exclusion region (162–166 GeV at 95% C.L.) was obtained for SM Higgs boson. With the increased statistics we will proceed to exclude wider mass range or to discover the Higgs. We are looking forward for continuing exciting physics results from the Tevatron experiments.

## 7 Acknowledgments

The autor would like to thank the organisers of the QUARKS-2010 International Seminar for invitation and hospitality, S. Denisov, D. Denisov, D. Bandurin, A. Dupperin for the useful discussions during the preparation for this seminar. This work was supported in part by RFBR grant No. 08-02-00607-a.

## References

- [1] F. Englert and R. Brout, Phys. Rev. Lett. 13, 321 (1964); P.W. Higgs, Phys. Rev. Lett. 13, 508 (1964).
- [2] LEP Electroweak Working Group, <http://lepewwg.web.cern.ch/LEPEWWG>.
- [3] LEP Collaborations (ALEPH, DELPHI, L3 and OPAL), Phys. Lett. B 565, 61 (2003).
- [4] H.E. Haber and G.L Kane, Phys. Rep. 117, 75 (1985).
- [5] DØ Collaboration, DØ Note 5972 (2009); CDF Collaboration, CDF Note 10068 (2010)
- [6] DØ Collaboration, DØ Note 5876 (2009); CDF Collaboration, CDF Note 9889 (2009)
- [7] FERMILAB-PUB-09-649-E-PPD (2010)
- [8] FERMILAB-PUB-10-017-E (2010); arXiv:1001.4162v3 [hep-ex] 2010
- [9] FERMILAB-CONF-09-557-E (2009)
- [10] CDF Collaboration, CDF Note 10105 (2010)
- [11] FERMILAB-FN-0851-E (2010); arXiv:1003.3363v2 [hep-ex] 2010
- [12] FERMILAB-TM-2439-E 2009; FERMILAB-TM-2460-E 2010
- [13] The LEP Collaborations: ALEPH, DELPHI, L3, OPAL and the LEP Electroweak Working Group, "A Combination of Preliminary Electroweak Measurements and Constraints on the Standard Model", arXiv:hep-ex/0612034 (2006).
- [14] arXiv:0804.4779 [hep-ph] (2008)
- [15] FERMILAB-PUB-09-644-E 2010; arXiv:0912.5104v2 [hep-ex] (2010)
- [16] FERMILAB-PUB-09-326-E 2009
- [17] M. Artuso et al., Eur. Phys. J. C57:309-492, (2008); G. Buchalla and A. J. Buras, Nucl. Phys. B400, 225 (1993); A.J. Buras, Phys. Lett. B 566, 115 (2003).
- [18] DØ Collaboration, DØ Note 5906 (2009); CDF Collaboration, CDF Note 9892 (2009)
- [19] Fermilab-Pub-10/114-E 2010
- [20] DØ Collaboration, DØ Note 5931 (2009)
- [21] arXiv:0912.0715v3 [hep-ex] (2010)
- [22] CDF Collaboration, CDF Note 9730 (2009)